A Compact 64-Pixel CsI(Tl)/Si PIN Photodiode Imaging Module With IC Readout

G. J. Gruber, W.-S. Choong, *Member, IEEE*, W. W. Moses, *Senior Member, IEEE*, S. E. Derenzo, *Fellow, IEEE*, S. E. Holland, *Member, IEEE*, M. Pedrali-Noy, *Member, IEEE*, B. Krieger, *Member, IEEE*, E. Mandelli, *Member, IEEE*, G. Meddeler, *Member, IEEE*, and N. W. Wang

***Abstract*—We characterize the performance of a complete 64-pixel compact gamma camera imaging module consisting of optically isolated $3 \times 3 \times 5$ mm^3 CsI(Tl) crystals coupled to a custom array of low-noise Si PIN photodiodes read out by a custom IC. At 50-V bias, the custom 64-pixel photodiode arrays demonstrate an average leakage current of 28 pA per 3×3 mm^2 pixel, a 98.5% yield of pixels with $<$100 pA leakage, and a quantum efficiency of about 80% for 540-nm CsI(Tl) scintillation photons. The custom 64-channel readout IC uses low-noise preamplifiers, shaper amplifiers, and a winner-take-all (WTA) multiplexer. The IC demonstrates maximum gain of 120 mV/1000 e$^-$, the ability to select the largest input signal in less than 150 ns, and low electronic noise at 8-μs peaking time ranging from 25 e$^-$ rms (unloaded) to an estimated 180 e$^-$ rms (photodiode load of 3 pF, 50 pA). At room temperature, a complete 64-pixel detector module employing a custom photodiode array and readout IC demonstrates an average energy resolution of 23.4% FWHM and an intrinsic spatial resolution of 3.3-mm FWHM for the 140-keV emissions of ^{99m}Tc. Construction of an array of such imaging modules is straightforward; hence this technology shows strong potential for numerous compact gamma camera applications, including scintimammography.**

***Index Terms*—Gamma camera, photodiode, scientimammography.**

I. Introduction

THE NEED for small, compact gamma cameras that can provide close proximity, high-quality single photon imaging of small organs has been motivated in recent years by the problem of breast cancer. For the 180 000 new breast cancer cases and 44 000 related deaths in the United States each year [1], [2], conventional Anger cameras have proven suboptimal in imaging tumors, in part because their large and bulky size prevents close access to desired imaging sites. The result is decreased spatial resolution, which implies decreased tumor detection sensitivity, a problem that could be lessened by compact camera design. Other small organ imaging applications, as well as applications involving surgical probes or the imaging of small animals, would also potentially benefit from compact gamma cameras.

A common approach to designing a compact gamma camera is to replace the bulky photomultiplier tubes (PMTs) with much more compact devices, either solid-state photodetectors[1] [3]–[6] or solid-state radiation detectors such as CdZnTe, which replace the scintillator in addition to the PMTs [7], [8]. The major technological challenge in implementing these designs is to achieve a system that matches Anger camera performance, particularly with regard to energy resolution, reliability, and cost. Silicon photodiodes have traditionally suffered from excessive electronic noise, HgI_2 photodiodes typically experience reliability problems, and CdZnTe remains an expensive material from which it is difficult to mass produce arrays of useful imaging size.

The solid-state detector (either photodiodes or CdZnTe) thus requires innovative development to achieve the material properties necessary to eliminate the PMTs. Further, the electronics readout must be made extremely dense to accommodate the large number of discrete pixels present in a reasonable imaging area. In this paper, we present a 64-pixel compact imaging module consisting of discrete CsI(Tl) crystals coupled to low-noise Si PIN (p-layer, intrinsic layer, n-layer) photodiodes, which are read out by a custom IC. This scales up our previous prototype work [4] from 12 to 64 pixels and presents a complete modular design that can be used to realize a variety of compact gamma camera configurations.

II. Module Components

The key components in the 64-pixel imaging module are presented in Fig. 1 along with their approximate sizes. The design revolves around making the module as compact as possible to optimize it for applications (such as scintimammography) that benefit from reduced imaging distances, a greater variety of views, and unique configuration possibilities such as using multiple cameras simultaneously.

The two critical innovations that make this feasible are the low-noise Si PIN photodiodes [9] and the custom IC readout [10]. The former replaces the bulky and expensive PMTs used in traditional Anger cameras, while the latter provides extremely dense processing of 64-pixel signals per 4.5×4.8 mm^2 IC.

Manuscript received November 5, 2000; revised August 9, 2001. This work was supported in part by the U.S. Department of the Army under Grant DAMD17-98-1-8302; by the Director, Office of Science, Office of Biological and Environmental Research, Medical Science Division of the U.S. Department of Energy under Contract DE-AC03-76SF00098; by the Laboratory Technology Research Division SC-32 (formerly ERLTT), Office of Science, U.S. Department of Energy, under a Cooperative Research and Development Agreement between Lawrence Berkeley National Laboratory and Capintec, Inc., Ramsey, NJ, under U.S. DoE Contract DE-AC03-76SF00098; by the National Institutes of Health, National Cancer Institute, under Grant R01-CA67911; and by the National Institutes of Health, National Heart, Lung, and Blood Institute, under Grant P01-HL25840.

The authors are with Lawrence Berkeley National Laboratory, Berkeley, CA 94720 USA (e-mail: wschoong@lbl.gov).

Publisher Item Identifier S 0018-9499(02)01650-7.

[1]For example, Model 2020tc Imager, Digirad Corporation, San Diego, CA (http://www.digirad.com).

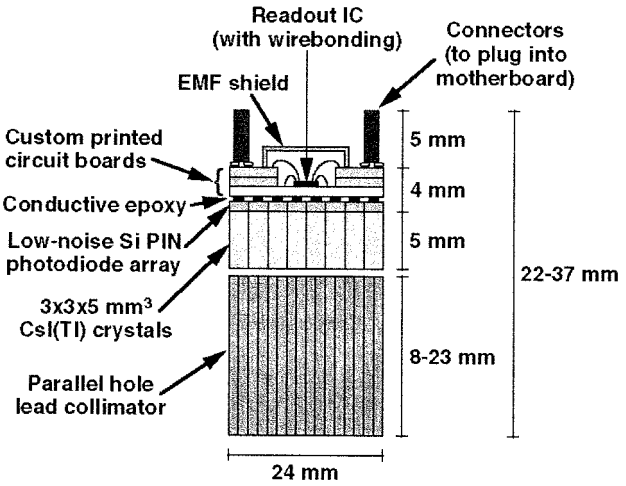

Fig. 1. Key components in a complete 64-pixel CsI(Tl) scintillator/Si PIN photodiode imaging module with custom IC readout. The total depth of the module depends on the collimator design but is less than 4 cm. A compact gamma camera constructed from an array of such modules need have a depth only slightly greater than that of the individual modules.

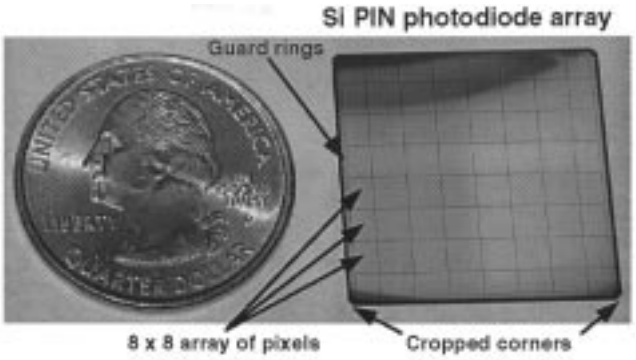

Fig. 2. Low-noise Si PIN photodiode array consisting of 64 3×3 mm^2 pixels, with a quarter (2.4 cm diameter) for scale. The side shown is the patterned p-layer, while the backside is the unpatterned, light-sensitive n-layer. A series of four guard rings encircle the array of pixels.

Since energy resolution is a prime concern, the electronic noise generated by both devices must be minimized. This is challenging because IC readout is typically noisy in comparison to discrete component readout, and photodiodes have lower gain (and thus lower signal-to-noise ratio) than PMTs. The low-noise photodiodes employed in these modules are the first reliable devices with sufficiently low room-temperature leakage current to provide adequate energy resolution for the applications under consideration.

Custom printed circuit boards are used to interface 1) the photodiode signals with the readout IC and 2) the readout IC with connectors, which allow external control of the module. The remainder of the module components are commercially available and include a high-sensitivity hexagonal hole lead collimator, an array of optically isolated $3 \times 3 \times 5$ mm^3 CsI(Tl) crystals, and shielding for the IC.

A. Silicon PIN Photodiode Arrays

A 64-pixel Si PIN photodiode array with 3×3 mm^2 elements and thickness of 300 μm is pictured in Fig. 2. A series of four guard rings run around the perimeter of the array to sink surface leakage current. The array is designed to maintain a 3-mm pitch between pixels when butted up against other arrays, so edge and corner pixels are slightly smaller than inner pixels. The corners of the arrays are cropped slightly in order to allow space for small wires to carry the 50-V bias around the edge of the array to the backside.

The goal in implementing the 64-pixel arrays was simply to replicate the 12-pixel prototype photodiode performance from [4] on a larger scale. This is challenging in part because if the yield for an individual pixel is y, then the yield for a perfect 12-pixel array is y^{12} while that for a 64-pixel array is much smaller at y^{64} (if the pixel yields are assumed to be uncorrelated). Since y is only about 80% for the 12-pixel prototype arrays, this presented a major problem. To increase the yield, a new process for depositing and annealing the phosphorus-doped polysilicon was developed: instead of deposition at 650 °C and no annealing, deposition was performed at 500 °C and followed by annealing at 600 °C. This increases the pixel yield significantly. The leakage current of the photodiodes is not noticeably affected, and as an added performance bonus the resistivity of the polysilicon is reduced by almost an order of magnitude.

Fig. 3 presents a histogram of the leakage currents of the pixels in 34 arrays, measured in darkness at room temperature under 50 V bias. The "good" pixels (those with less than 100 pA leakage current) demonstrate an average current of 28 ± 7 pA, about an order of magnitude better than the best commercial Si photodiode arrays presently available. The guard rings of all 34 arrays exhibit an average current of 1.7 ± 0.4 nA. Using the 100-pA metric, the yield for individual photodiode elements is 2143 of 2176, or $y = 98.5\%$. This provides a respectable y^{64} of 38%, which is consistent with the observed yield of 41% (14 of 34) flawless arrays. Further, if one "bad" (i.e., high leakage current) pixel per array is acceptable, then the measured array yield increases to 74% (25 of 34).

The photodiodes are optimized for the 540-nm scintillation photons of CsI(Tl) with a 67.9-nm-thick antireflective layer of indium–tin–oxide (ITO), yielding a quantum efficiency of about 80%. Finally, the photodiodes demonstrate the expected capacitance of about 3 pF per pixel.

B. Custom IC Readout of Photodiodes

The readout IC is described in detail in [10]. It is a mixed analog–digital design fabricated in CMOS (HP 0.5-μm 3.3-V technology) and covering an area of 4.5×4.8 mm^2. Its front end is an array of 64 analog input channels consisting of charge-sensitive preamplifiers and shaper amplifiers, the behavior of which can be adjusted with external signals. The noise performance of the front end has been optimized for these photodiodes, and at 8-μs peaking time [appropriate for CsI(Tl) scintillation], the performance ranges from 25 e$^-$ rms when unloaded to an estimated 180 e$^-$ rms with a photodiode load (3 pF, 50 pA). The IC provides a maximum gain of 120 mV/1000 e$^-$. Prototype versions of the front end are described in [11].

The remainder of the IC is dominated by the "winner take all" (WTA) circuitry. This section reduces the 64 amplified, shaped signals to a single "winner" channel by constantly selecting the channel with the greatest amplitude. The end result is that

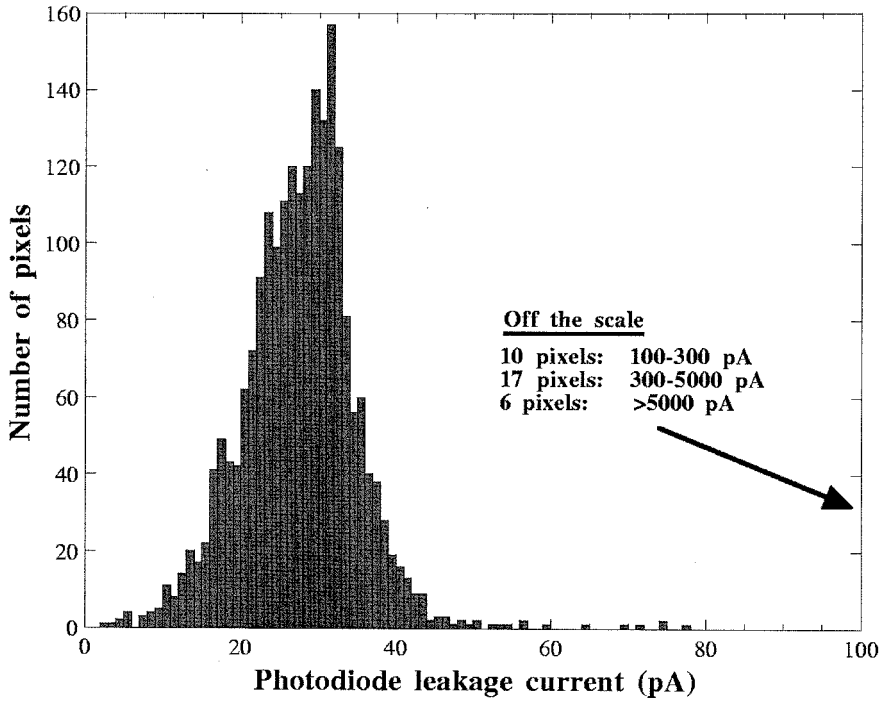

Fig. 3. Histogram of the leakage current values for pixels in 34 64-pixel arrays. Histogram bins are 1 pA wide. Photodiodes are 3×3 mm^2 in size and were in the dark at room temperature under a 50-V bias. The pixels with leakage current less than 100 pA (2143 out of 2176) demonstrate an average current of 28 ± 7 pA.

64 analog input lines are reduced to a single analog output line plus six digital bits, which identify the location of the winning channel. The IC is able to select the largest input signal and generate the corresponding 6-bit address in less than 150 ns. Careful layout of the WTA circuitry is crucial since feedback of digital noise into the sensitive preamplifiers could result in chip failure. Prototype versions of the WTA circuitry are described in [12].

III. Design Choices

A number of key design decisions were made in the course of developing the 64-pixel imaging modules. These choices are targeted at producing modules that are viable as the building blocks for compact gamma cameras useful for scintimammography and other applications. To that end, tradeoffs were selected that provide good performance while producing devices that can be constructed and assembled into a modular array in a straightforward and reasonably inexpensive fashion.

A. Compactness and Dead Area

The major advantages of this technology revolve around providing compactness, so this needs to be exploited to the fullest. As is evidenced in Fig. 1, the majority of the module depth is taken up by the collimator and the CsI(Tl), which cannot be made significantly smaller. The electronics readout—including the custom printed circuit boards, the IC, and the connectors for plugging into a motherboard—are less than 1 cm in depth, much of which is the height of the connectors.

By maintaining virtually no camera dead area, the number of useful clinical views this technology can provide is increased. No module components extend beyond the active area of the 64-pixel array, so multiple modules can be butted up against each other with little or no dead area in between or at the edges of the camera. Dead area at the camera periphery, then, will be determined solely by the thickness of the packaging and lead shielding. Note that the photodiodes (Fig. 2) are designed to provide 3-mm pitch between all pixels, even those on different arrays. The slightly smaller edge and corner pixels employed to achieve this do decrease signals levels in those pixels, but since the corresponding CsI(Tl) crystals are still full size, there is no introduction of imaging dead area or loss of sensitivity.

B. Pixel Size

Monte Carlo simulations were conducted in [13], which suggest that decreasing pixel size much below 3×3 mm^2 offers little advantage in imaging breast tumors. This is not surprising given that collimator spatial resolution—not the intrinsic spatial resolution determined by pixel size—is typically the limiting factor in such medical applications. Further, since the size of the tumors that can be successfully imaged with gamma cameras is generally significantly larger than 3 mm, small pixel size is not critical. Decreasing pixel size (and therefore the area of a 64-pixel module) does, however, significantly increase the density of the readout electronics, making it challenging to fit all the electronics within the same area as the pixel array. This increases complexity and expense (more modules are now required to cover the same area) and may result in less compact devices. Hence 3×3 mm^2 pixels were employed.

C. Cooling of Photodiodes

Obtaining the $\sim$9% full-width at half-maximum (FWHM) energy resolution offered by conventional Anger cameras at 140 keV has historically been challenging with CsI(Tl)/Si photodiode technology. One potential means of improving energy resolution is to cool the photodiodes to about 5 °C in

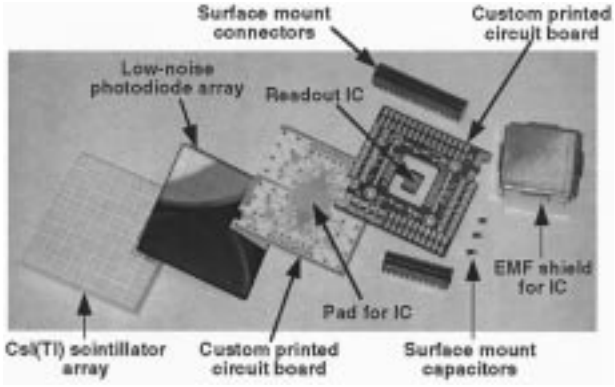

Fig. 4. Complete but unassembled 64-pixel module. The CsI(Tl) and low-noise photodiode array are coupled together with transparent epoxy. The photodiodes connect to the custom printed circuit boards via carefully applied drops of conductive epoxy. The readout IC is wirebonded to the printed circuit boards, which support the IC by routing input signals from the photodiodes, control signals from the connectors, and output signals generated by the IC.

order to lower leakage current and therefore electronic noise. While a room-temperature energy resolution of 10.7% FWHM at 140 keV was observed in [4], a cooled environment lowered the figure to 7.5% FWHM at 122 keV for similar technology [5]. However, the Monte Carlo simulations in [12] suggest that small improvements in energy resolution do not significantly improve breast tumor imaging as the main background is not scattered but unscattered emissions from nonspecific uptake in normal breast tissue. Therefore, the 64-pixel module described in this paper is designed to be operated at room temperature, avoiding the added complexity, size, and expense of a cooling system. Should energy resolution improvements prove necessary in the future, however, a cooling system remains a possibility.

D. Collimation

Although any collimator could be attached in front of the detector module, the intent is to use a high-sensitivity hexagonal hole lead collimator. Again, the simulations in [13] suggest that high sensitivity is more advantageous than high resolution and that hexagonal holes perform comparably to square holes. As new collimator technology advances, however, it may become preferable to use a square hole tungsten laminate collimator wherein the square holes are matched to the individual pixels. Matching more than one hole to each pixel (e.g., 4-to-1 or 9-to-1) offers the possibility of an extremely compact collimator.

IV. Module Performance

A. Module Assembly

A complete 64-pixel module immediately prior to the final assembly steps is depicted in Fig. 4. Assembly of the components requires a series of steps during which multiple epoxies are applied, wirebond connections are made, and surface mount components are soldered into place. Key challenges during assembly revolve around the very sensitive photodiode array and readout IC, including avoiding mechanical, chemical, or thermal damage to them, and providing them with all necessary wirebond and conductive epoxy electrical connections.

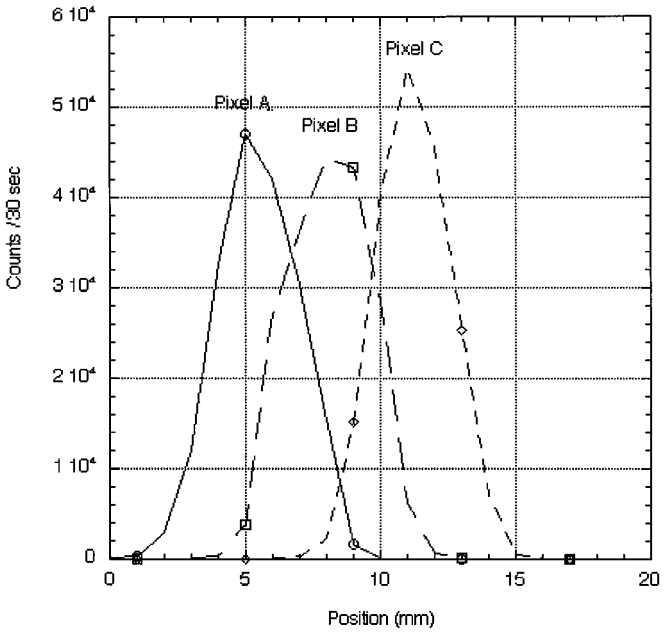

Fig. 5. Response of three individual pixels to a 2.5-mm-diameter ^{57}Co collimated beam scanned across the face of the CsI(Tl) array. The average spatial resolution is 3.3-mm FWHM.

B. Intrinsic Spatial Resolution

When scanning a 2.5-mm-diameter collimated ^{57}Co beam across several crystals in the central region of the CsI(Tl) array, we observe an average intrinsic spatial resolution of 3.3-mm FWHM. Given the size of the source, this resolution is consistent with the crystal size of 3 mm. The responses of three individual pixels are displayed in Fig. 5. This intrinsic spatial resolution suggests that the system spatial resolution of a high-sensitivity imaging system employing these modules will be determined primarily by the collimator geometry.

C. Energy Resolution

Typical pulse-height spectra for corner, edge, and inner channels excited by the 140-keV emissions of ^{99m}Tc are shown in Fig. 6. Histograms of the energy resolution demonstrated by border (edge plus corner pixels) and inner pixels in a single 64-pixel module are shown in Fig. 7. The average energy resolution for border and inner pixels is 25.6% and 21.9% FWHM, respectively, while the average across the entire module is 23.4% FWHM. The signal-to-noise ratio of the border pixels is slightly lower than the inner pixels because the border pixel of the photodiode array has a smaller area, resulting in a lower signal when coupled to the CsI(Tl) array. However, the electronic noise of the border pixels is lower than that of the inner pixels because of the lower capacitance and leakage current.

While the energy resolution of our first 64-pixel module is not as good as the 10.7% that has been achieved with the smaller

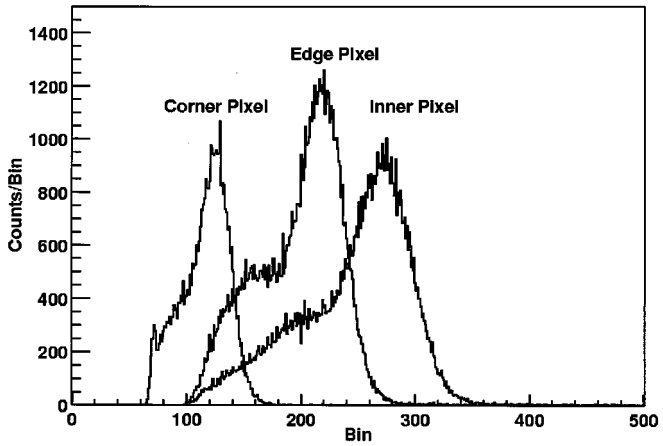

Fig. 6. Room-temperature pulse-height spectra for typical corner, edge, and inner pixels excited by 140-keV emissions of ^{99m}Tc. The energy resolutions of the corner, edge, and inner pixels are 23.0%, 19.8%, and 20.4% FWHM, respectively.

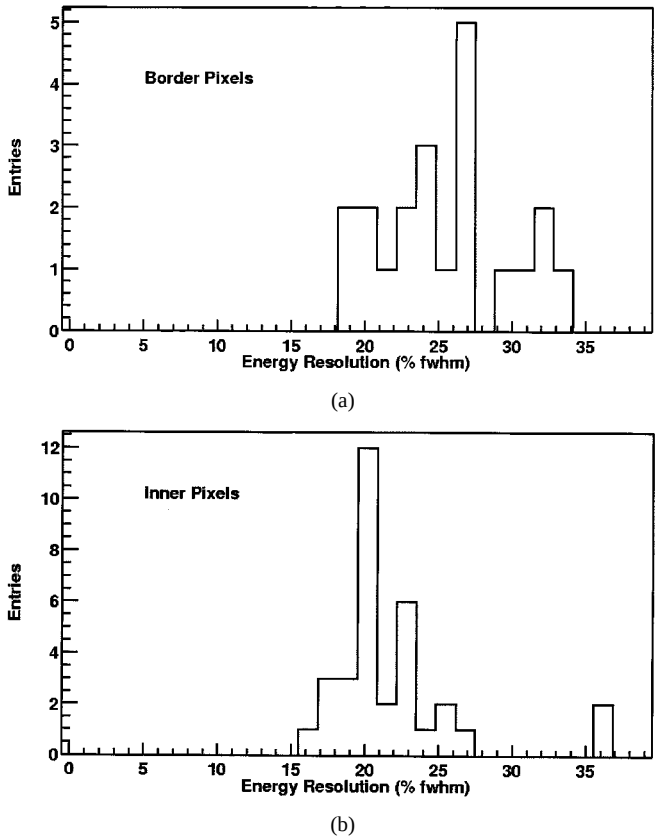

Fig. 7. Histograms of energy resolution demonstrated by (a) individual border and (b) inner pixels in the 64-pixel module. The average energy resolutions for the border and inner pixels are 25.6% and 21.9% FWHM, respectively.

prototype detectors in [4] and [5], it demonstrates that the technology has been successfully scaled up to 64 pixels while maintaining a reasonable energy resolution.

We have partially investigated the reasons for this performance degradation. Although the electronic noise is slightly higher (possibly due to higher photodiode leakage current), the signal level is significantly lower. However, the photodiode quantum efficiency, scintillator light output, and amplifier gain are all comparable to (or slightly lower) than that of the earlier components. The scintillation light collection efficiency exhibits more depth dependence, which degrades the energy resolution without significantly affecting the light output, yet this effect is not large enough to cause the observed degradation. It is possible that the signal is attenuated, either optically (by passivation layers on the photodiode or the glue used to couple it to the scintillator) or electrically (by the conductive epoxy, wirebonds, etc.).

V. Conclusion

This compact gamma camera technology has been scaled up to 64-pixel imaging modules. The key and innovative advances in the development of the 64-pixel compact imaging modules are 1) the IC, which allows efficient readout of many channels, and 2) the low leakage current Si PIN photodiodes, which can potentially replace traditional PMTs without introducing unacceptably high electronic noise. As individual components, both devices behave to expectations and contribute to a highly compact imaging module with virtually no dead area. In addition to the emphasis on compactness, the module has been designed so that an array of such devices can be assembled to form a complete compact gamma camera of useful imaging area.

At room temperature, our first 64-pixel module demonstrates an intrinsic spatial resolution of 3.3-mm FWHM and an energy resolution of 23.4% FWHM (border pixels demonstrate an energy resolution only about 17% larger than the energy resolution of inner pixels). The intrinsic spatial resolution meets expectations and suggests that when a high-sensitivity collimator is employed, system spatial resolution will be determined primarily by the collimator geometry. The energy resolution, however, is significantly worse than the 10.7% FWHM that prototype work has shown is achievable, and therefore future efforts will strive to improve this performance. Most of the difficulties with energy resolution likely lie in the module assembly steps, which can subtly damage either the sensitive photodiode array or the readout IC.

Another future direction for this work involves constructing a multimodule camera and characterizing its performance as a medical imaging device. This involves the design and fabrication of a motherboard that the individual modules are plugged into and that interfaces with a data-acquisition computer, a project already under way for a 4×4 16-module design.

Acknowledgment

The authors thank Dr. T. F. Budinger for his advice regarding this research. They further thank C. S. Tindall for processing the photodiode arrays, M. H. Ho for his contributions in the lab, and G. J. Zizka for his extensive wirebonding efforts.

References

[1] J. R. Harris, M. E. Lippman, U. Veronesi, and W. Willett, "Breast cancer," *New Eng. J. Med.*, vol. 327, pp. 319–328, 1992.
[2] S. L. Parker, T. Tong, S. Bolden, and P. A. Wingo, "Cancer statistics," *Cancer J. Clinicians*, vol. 47, pp. 319–328, 1997.
[3] J. Strobel, N. H. Clinthorne, and W. L. Rogers, "Design studies for a cesium iodide silicon photodiode gamma camera," *J. Nucl. Med.*, vol. 38, p. 31P, 1997.

[4] G. J. Gruber, W. W. Moses, S. E. Derenzo, N. W. Wang, E. Beuville, and M. H. Ho, "A discrete scintillation camera module using silicon photodiode readout of CsI(Tl) crystals for breast cancer imaging," *IEEE Trans. Nucl. Sci.*, vol. 45, pp. 1063–1068, 1998.

[5] B. E. Patt, J. S. Iwanczyk, C. Rossington Tull, N. W. Wang, M. P. Tornai, and E. J. Hoffman, "High resolution CsI(Tl)/Si-PIN detector development for breast imaging," *IEEE Trans. Nucl. Sci.*, vol. 45, pp. 2126–2131, 1998.

[6] M. P. Tornai, B. E. Patt, J. S. Iwanczyk, C. S. Levin, and E. J. Hoffman, "Discrete scintillator coupled mercuric iodide photodetector arrays for breast imaging," *IEEE Trans. Nucl. Sci.*, vol. 44, pp. 1127–1133, 1997.

[7] J. F. Butler, C. L. Lingren, S. J. Friesenhahn, F. P. Doty, W. L. Ashburn, and R. L. Conwell *et al.*, "CdZnTe solid-state gamma camera," *IEEE Trans. Nucl. Sci.*, vol. 45, pp. 1158–1165, 1998.

[8] M. Singh and E. Mumcuoglu, "Design of a CZT based BreastSPECT system," *IEEE Trans. Nucl. Sci.*, vol. 45, pp. 1158–1165, 1998.

[9] S. E. Holland, N. W. Wang, and W. W. Moses, "Development of low noise, back-side illuminated silicon photodiode arrays," *IEEE Trans. Nucl. Sci.*, vol. 44, pp. 443–447, 1997.

[10] M. Pedrali-Noy, G. J. Gruber, B. Krieger, E. Mandelli, G. Meddeler, and W. W. Moses *et al.*, "PETRIC—A positron emission tomography readout integrated circuit," *IEEE Trans. Nucl. Sci.*, vol. 48, pp. 479–484, 2000.

[11] W. W. Moses, I. Kipnis, and M. H. Ho, "A 16-channel charge sensitive amplifier IC for a PIN photodiode array based PET detector module," *IEEE Trans. Nucl. Sci.*, vol. 41, pp. 1469–1472, 1994.

[12] W. W. Moses, E. Beuville, and M. H. Ho, "A winner-take-all IC for determining the crystal of interaction in PET detectors," *IEEE Trans. Nucl. Sci.*, vol. 43, pp. 1615–1618, 1996.

[13] G. J. Gruber, W. W. Moses, and S. E. Derenzo, "Monte Carlo simulation of breast tumor imaging properties with compact, discrete gamma cameras," *IEEE Trans. Nucl. Sci.*, vol. 46, pp. 2119–2123, 1999.